Donahue, R., Hardin, R., and Beckermann, C., "Effect of Gating System and Pour Order on Steel Casting Cleanliness," in Proceedings of the 76th SFSA Technical and Operating Conference, Paper No. 3.4, Steel Founders' Society of America, Chicago, IL, 2022.

Effect of Gating System and Pour Order on Steel Casting Cleanliness

Robert Donahue, Richard A. Hardin and Christoph Beckermann

Solidification Laboratory
Department of Mechanical Engineering
The University of Iowa, Iowa City, 52242

Abstract

Oxide inclusions are one of the major defects observed in steel casting and contribute to large repair costs and production delays. The effect of the gating system and pour order on casting cleanliness is investigated in an experimental study. Two different gating systems are selected from a previous study. The first gating system is poor and employs a standard pouring cup, oversized sprue and runner, and a side ingate near the top. The second gating system is more sophisticated and features an offset pouring basin, a tapered sprue, streamlined runner connections, and a tapered bottom ingate. A total of 36 castings are produced, 18 for each of the two gating systems. The castings are filled using a tilt pour ladle that has a capacity for 6 molds. Inclusion coverage is measured on the chilled cope surface of the rectangular block that constitutes the casting. It is found that the more sophisticated gating system offers a 2.5 times improvement in the inclusion area percentage relative to the poor gating system. This is attributed to more of the oxides from the ladle being trapped by the pouring basin and the rest of the gating system. Furthermore, the poor gating system results in a strong dependence of the casting cleanliness on the pour order, with the first casting having an inclusion area percentage that is about twice as high as the sixth. This dependency is much reduced for the sophisticated gating system. Heat to heat variations in casting cleanliness are found to be negligibly small in the present study.

Introduction

Oxide inclusions in steel castings are estimated to contribute 20% to the cost of a casting due to the costs of removing them and repairing the casting [1]. They are also a frequent cause of premature failure of steel castings when not detected during production. There are numerous sources of oxides such as the ladle lining and poorly deoxidized melt, and many casting process variables can affect the levels of oxides in steel castings. The cleanliness of the melt can vary from heat to heat, so called dirty heat versus clean heat, due to poor control of the melt practice. Considering all the sources of oxide inclusions, reoxidation inclusions, formed during pouring of the metal into the mold, are a common cause of inclusion defects in steel castings, if not the most common. Reoxidation inclusions form when deoxidized steel comes into contact with oxygen during mold filling. They are reported to make up 83% of oxide inclusions in low-alloy steel castings and 48% of inclusions found in high-alloy steel castings [2]. Reoxidation of the steel during pouring can be minimized by employing well-designed gating systems. Much research has been performed for over 50 years to establish rules for gating castings. However, the design of gating systems is still more of an art than a science.

In 2021, the current authors presented an experimental study on the effects of the gating system and casting geometry on oxide inclusions in steel castings [3]. An important finding was that almost no inclusions were generated inside the gating system, including the downsprue and runner. This was determined by locating filters in such a way as to isolate the sources of the inclusions. It was found that the primary source of inclusions was from the ladle and, to a much lesser extent, the pouring cup. Even though hardly any inclusions were found to be generated inside the gating systems, it cannot be said that the gating system has no effect on inclusions in a casting. The gating system still has two effects: (i) it "filters" out inclusions from the ladle if, for example, inclusions can float out or get stuck and trapped inside the gating system prior to entering the casting; (ii) inclusions are not evenly distributed in a casting and the location and geometry of the gating system will affect the distribution in the casting.

The present study is a continuation of the above 2021 experiments on the effects of the gating system on oxide inclusions in steel castings. Two gating systems, Cases A and E, were selected from Reference [3] to address in detail the following three questions:

(i) What is the actual improvement in casting cleanliness when switching from a poor gating system with a standard pouring cup, an oversized sprue and a side ingate near the top (Case A) to a more sophisticated gating system with an offset pouring basin, a tapered sprue, rounded runner connections, and a tapered bottom ingate (Case E)?

(ii) What is the effect of pour order on casting cleanliness when using a standard tilt pour ladle that has the capacity to fill six castings?

(iii) How does casting cleanliness vary between different heats?

There are two key aspects in the current experiments that are adopted from Reference [3]. First, the casting itself is a simple rectangular block without any risers. This enables the measurement of all oxide inclusions entering from the gating system, without an unknown and variable portion of the inclusions being hidden inside a riser. A chill is used on the top of the block to create a flat cope surface (without shrinkage pipe or depression) on which the inclusions can be easily detected. Second, the oxide inclusions are measured in a quantitative fashion, rather than by assessing casting cleanliness through a qualitative rating system. Three different inclusion measurement methods were developed in Reference [3]. The first method, based on radiographs, is not employed in the current study. The second and third methods are used here and, for completeness, are reviewed in the next section. The experiments of the present study are described in the ensuing section, which is followed by the presentation and discussion of the results.

Inclusion Measurement Methods

Three inclusion measurement methods were developed by the present authors in Reference [3]. They all rely on the fact that all but the smallest oxide inclusions float to the cope surface of a casting before significant solidification of the steel commences. In the first method, quantitative analysis of radiographs was used to measure the inclusion indications present in the uppermost ½" thick section of a casting's cope surface. In the second method the as-cast cope surface is inspected, and inclusions are marked. In the third method the cope surface is blasted with media, cleaning it to expose inclusion pits, and then inspected and inclusions marked. In both the second and third methods, the marked areas of inclusions are digitized and quantitatively analyzed using image analysis software. The second and third methods are adopted in the present study and their procedures are described in more detail below.

Inclusion Measurement Method 2: Quantitative Image Analysis of As-Cast Surface

In this inclusion measurement method, surface inspection and image analysis are performed. The inclusions on the as-cast surface are identified, as shown in the four “inclusion examples” images in Figure 1. After identifying the inclusions on the as-cast cope surface (lower left image in Figure 1), envelopes are marked and filled in at each inclusion using *Paint 3D* software as shown in Figure 1. This image is then converted to a binary format (“processed binary image” in Figure 1) to obtain a black and white inclusion map. From the inclusion map, the area of the marked indications is measured using the image analysis software *Fiji* [4]. Some filtering is performed as mentioned in the lower right of Figure 1. After this, the number of discrete inclusion indications, the indication size distribution, and the total indication area fraction on the casting surface are determined using *Fiji*. Some example results are provided in the bottom right of Figure 1.

Inclusion Measurement Method 3: Analysis of Media Blasted Surface, “Pit Method”

This method is similar to Method 2, except that the as-cast cope surface undergoes media blasting before inspection. This was performed to improve the inspection by reducing uncertainties in determining whether indications on the casting surfaces are inclusions, or if they are caused by some other casting surface phenomenon (mold-metal reaction, scale, cold laps, flow lines etc.). An example of the before/after media blasting of a cope surface is shown in the two upper left images in Figure 2. It was found that the media blasted surfaces gave clearer evidence of inclusions. The main identifying feature of inclusions on the casting surfaces were found to be pits, which are visible under the inclusion location after blasting the surface and removing the inclusion (see “examples of inclusion pits” images in Figure 2). Since these pits go hand-in-hand with the inclusions, they were used to identify inclusion areas on the experimental casting surfaces, and to distinguish between inclusions and other surface indications such as cold lapping and scale. The inclusion locations are marked by hand with a dot on the cope surface and then photographed (lower left image in Figure 2). The inclusion pits in the photo are digitally marked with an envelope in *Paint 3D* (lower middle image in Figure 2), and converted to the “processed binary image” or inclusion map as shown in the lower rightmost image in Figure 2. Like in Method 2, *Fiji* is then used to measure the number of discrete inclusion indications, the indication size distribution, and the total indication area fraction on the casting surface.

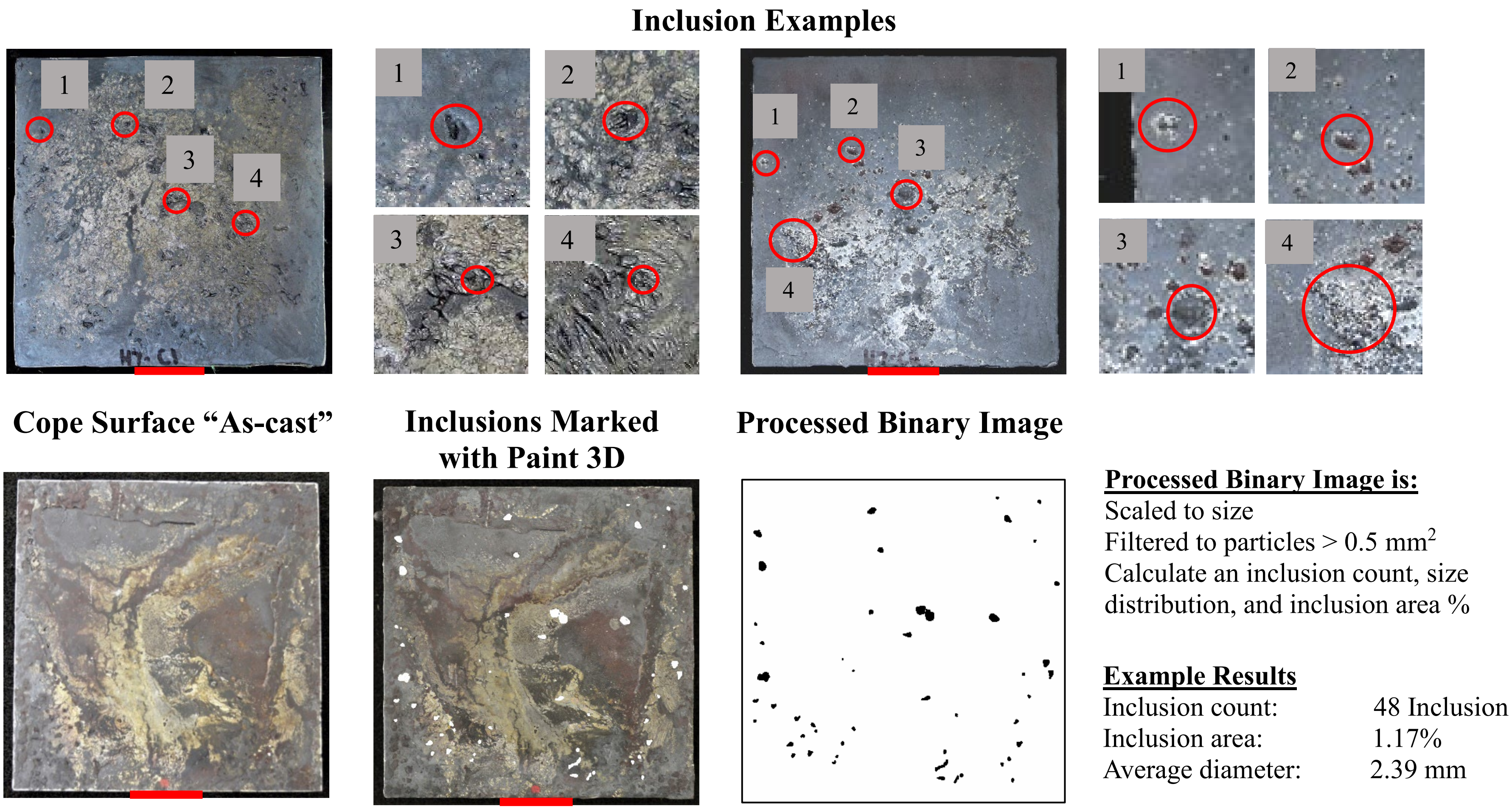

Figure 1. Images to assist the reader in understanding inclusion measurement Method 2, as-cast surface analysis. The casting surface is inspected without any cleaning or preparation. Inclusion examples illustrate indications that are counted using this method. Inclusions are identified and marked. A binary image is generated and used to measure the number of inclusions, size distribution and total inclusion area % on the surface using image analysis.

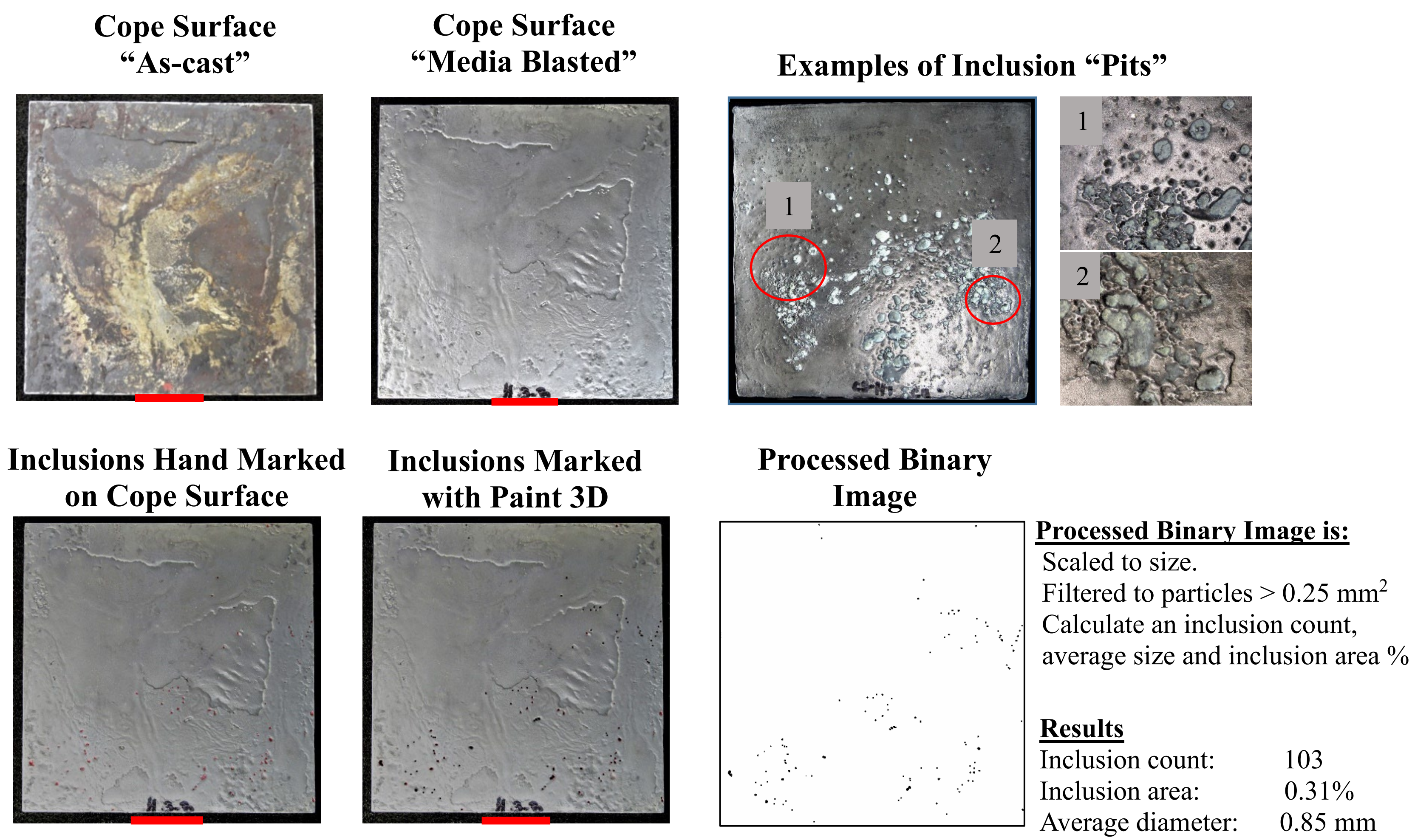

Figure 2. Images to assist the reader in understanding inclusion measurement Method 3, "pit" analysis. The casting surface has been media blasted to open up surface pits before inspection. Examples of the pit indications that are counted using this method. The pits are identified and marked. A binary image is generated and used to measure the number of inclusions, size distribution and total inclusion area % of the surface using image analysis.

Description of Experiments

Figure 3 shows the design of the castings for Cases A and E, including their main dimensions and weights (see also Reference [3]). In both cases, the casting itself is a 6” x 6” x 3” rectangular block. The cope is covered by a 8” x 8” x 1” chill to create a flat casting surface on which the oxide inclusions can be measured. By machining a test casting in small layers from the top, it was verified that all inclusions larger than about 0.4 mm in diameter float to the cope surface before significant solidification commences [3]. For Case A, the gating system consists of a pouring cup, a cylindrical straight sprue, a runner with a rectangular cross section, and an ingate located on the side of the block near the top. Computer simulations of the filling process indicated that the sprue and runner are oversized, in that they do not fill with liquid steel before the casting block is full. For Case E, the gating system consists of an offset pouring basin, a tapered sprue, a cylindrical runner that is connected to the sprue and the ingate through round elbows, and a tapered bottom ingate. Simulations showed that during the majority of the filling process, the gating system for Case E is filled with liquid metal and that no fountaining occurs near the ingate. Thus, air entrainment is minimized. All molds were 3D printed at the University of Northern Iowa Additive Manufacturing Center.

In all experiments, ASTM A216 WCB steel was poured using a tilt pour ladle at the University of Northern Iowa Metal Casting Center. A photo of the ladle is included in Figure 3. The ladle contains an entire heat (approximately 300 lb.) and is large enough to pour 6 of the present block castings. During pouring, a stream of liquid steel was formed by a rounded lip at the top edge of the ladle.

A total of 36 castings were poured, with an equal number of Case A and Case E castings. The castings were poured from 6 different heats, labeled Heat 9 to 13 (Heats 1 through 8 were poured as part of the experiments in Reference [3]). The experimental matrix of cases is shown in Figure 4. The first heat consisted entirely of Case A castings, while the second heat was all Case E castings. The other four heats had an equal number of Case A and E castings (3 each), with the pour order randomized.

A video of each pouring process was made. The fill times, the stream diameters and angles at the top of the pouring cup or basin, and the approximate impact location of the stream from the ladle were determined from the video and are summarized in Figure 5. The pouring process was stopped as soon as the pouring cup or basin started filling with liquid steel. The fill times for the Case A and E castings were about 8 s and 10 s, respectively.

Casting Block

Volume: 108.0 in^3

Weight: 30.7 lbs.

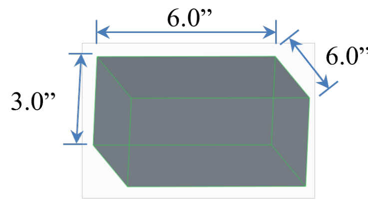

Case A

Straight sprue, 1.0” dia.

Rect. ingate

1.2” wide x 0.65” tall

Gating 1:1:1

Total Weight – 41.7 lbs.

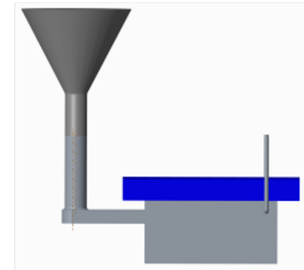

Chill Plate

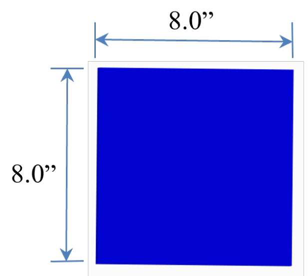

1.0” thick

Case E

Tapered sprue:

Top 1.0” dia.

Bottom 0.75” dia.

Fill basin

Bottom center ingate

Total Weight – 59.1 lbs.

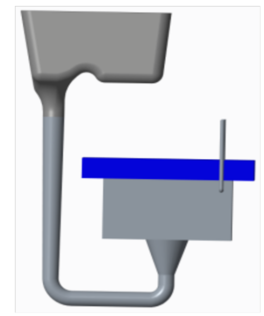

Figure 3. Picture of the tilt pour ladle used to fill the test castings. Design features and dimensions of the castings for Cases A and E.

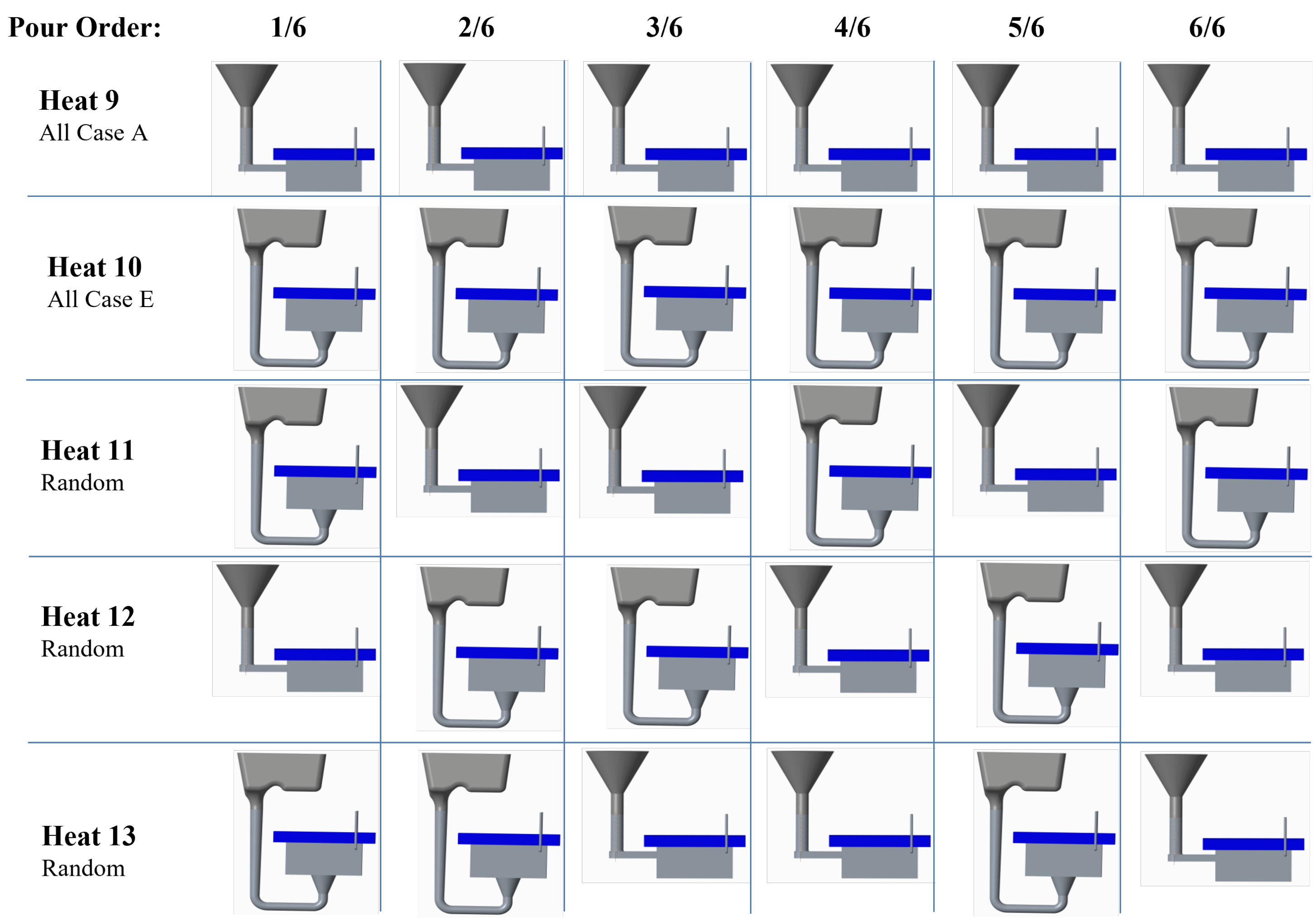

Figure 4. Test matrix used in the present experiments.

Heat 9	Pour Time (s)	Stream Diameter (in)
Case A	6.0	1.00
Case A	8.0	1.00
Case A	7.0	1.00
Case A	7.0	1.00
Case A	8.0	1.25
Case A	6.5	0.75
Heat 10		
Case E	10.0	0.80
Case E	9.0	0.75
Case E	10.0	0.75
Case E	10.0	0.60
Case E	10.0	0.70
Case E	7.0	0.60
Heat 11		
Case E	7.0	1.50
Case A	9.0	1.25
Case A	9.0	1.00
Case E	9.0	0.75
Case A	8.0	1.00
Case E	10.0	1.25
Heat 12		
Case A	6.0	0.90
Case E	8.0	0.80
Case E	8.0	0.70
Case A	6.0	0.90
Case E	9.0	0.70
Case A	11.0	0.90

Heat 13	Pour Time (s)	Stream Diameter (in)
Case E	8.0	0.80
Case E	9.0	0.90
Case A	8.0	0.80
Case A	7.0	0.70
Case E	12.0	0.60
Case A	8.0	0.70

Typical stream location and angle

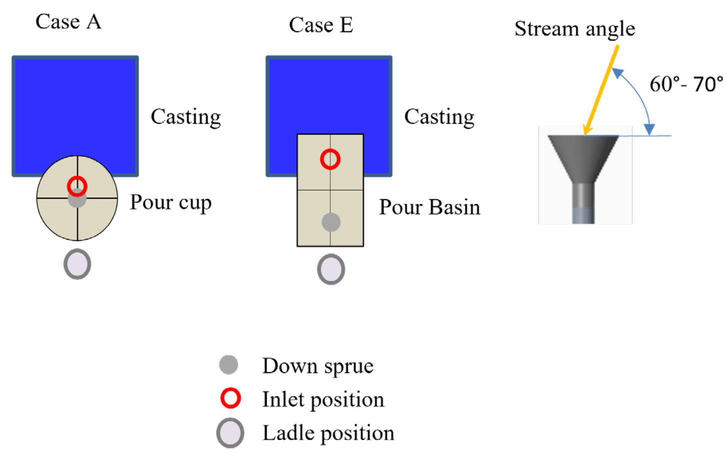

Figure 5. Pour related data obtained from the casting process videos.

Experimental Results

Images of the cope surfaces of the blocks cast from Heats 9 (all Case A) and 10 (all Case E) are provided in Figures 6 and 7. Figure 6 shows the as-cast surfaces that were used for inclusion measurement Method 2, together with the resulting digitized inclusion maps. It can immediately be observed that the Case A castings show larger areas of inclusions than the Case E castings. Furthermore, in both cases the inclusion coverage continually decreases with the pour number increasing from 1 to 6. In other words, the first casting poured from a heat is considerably "dirtier" than the last casting. Figure 7 shows the media blasted cope surfaces from Heats 9 and 10 that were used for inclusion measurement Method 3, together with the resulting digitized inclusion maps. It can be seen that the inclusion pits closely correspond to the as-cast indications in Figure 6.

For completeness, the measured inclusion maps for all heats and casting cases are provided in Figures 8 and 9. Figure 8 shows the maps for inclusion measurement Method 2 and Figure 9 for Method 3. The Case A maps have a red frame and background, while the Case E maps are in blue. Considerable variations in the inclusion coverage can be observed between the various cases. The indication area percentages obtained from these maps are summarized in Figure 10. They vary from as high as 32% to as low as 1.4%. These results are statistically analyzed in the next section.

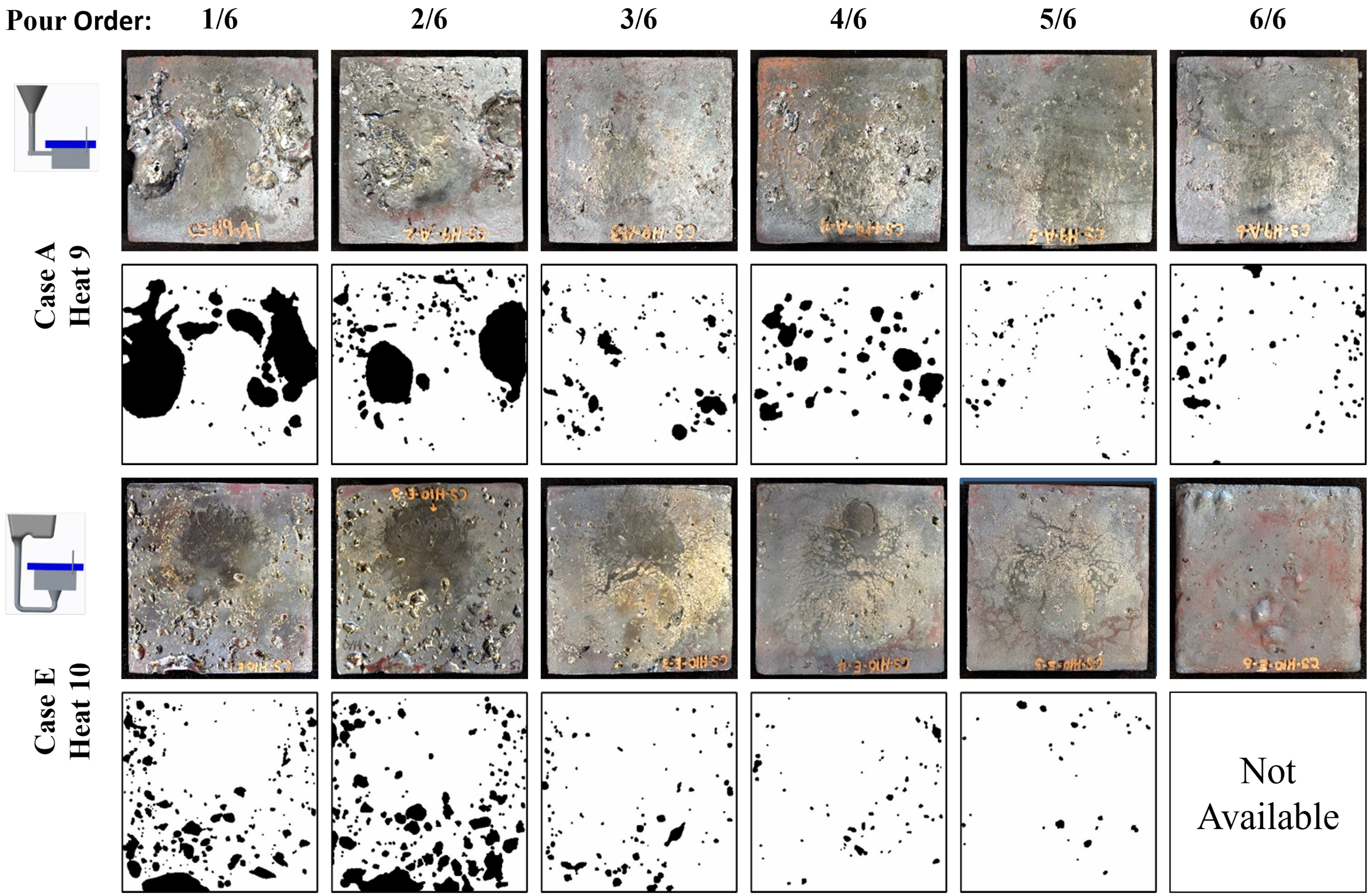

Figure 6. Images of the as-cast cope surfaces for Heats 9 (all Case A castings) and 10 (all Case E castings), together with the corresponding digitized inclusion maps obtained using Method 2.

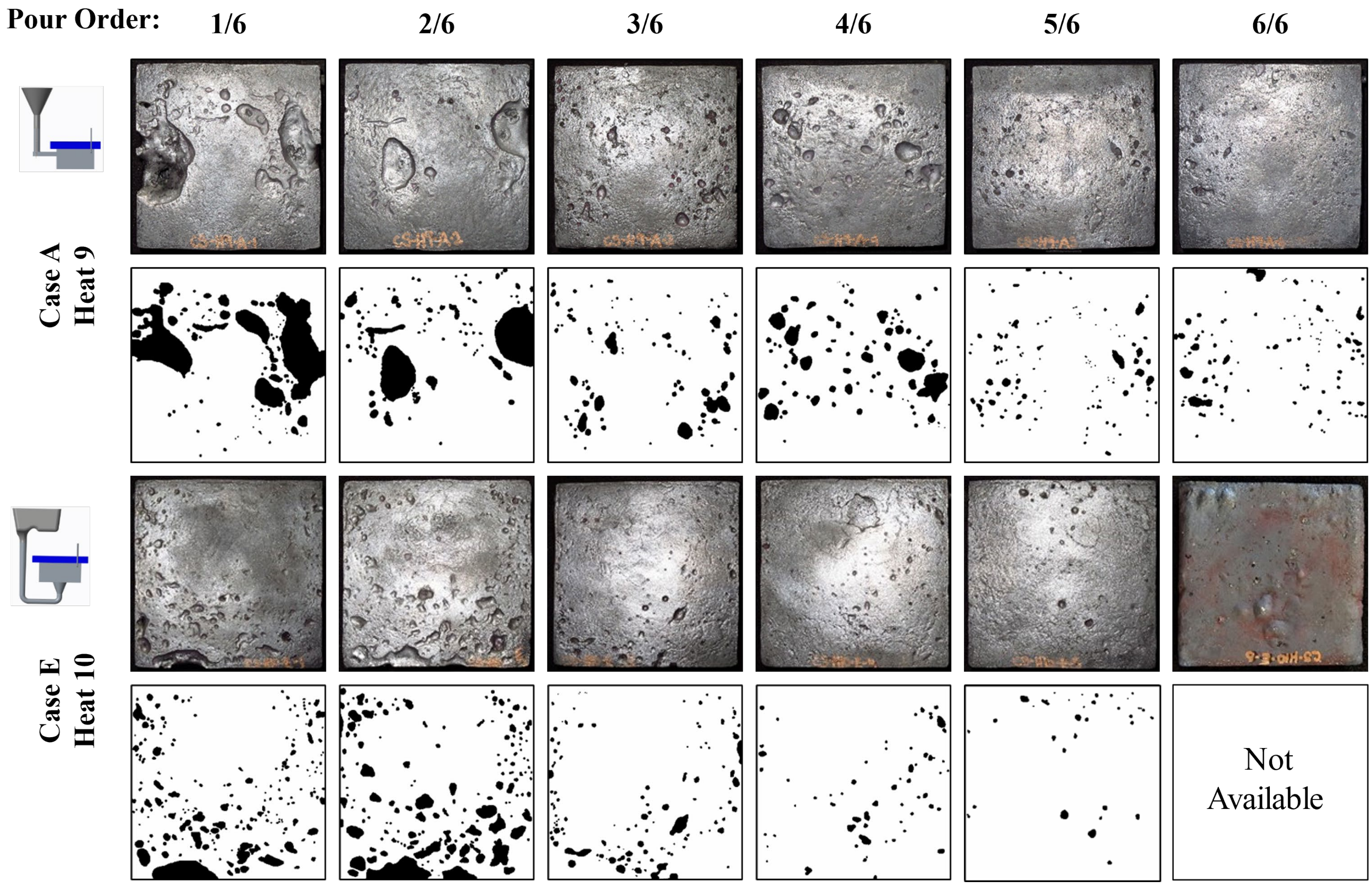

Figure 7. Images of the media blasted cope surfaces for Heats 9 (all Case A castings) and 10 (all Case E castings), together with the corresponding digitized inclusion maps obtained using Method 3.

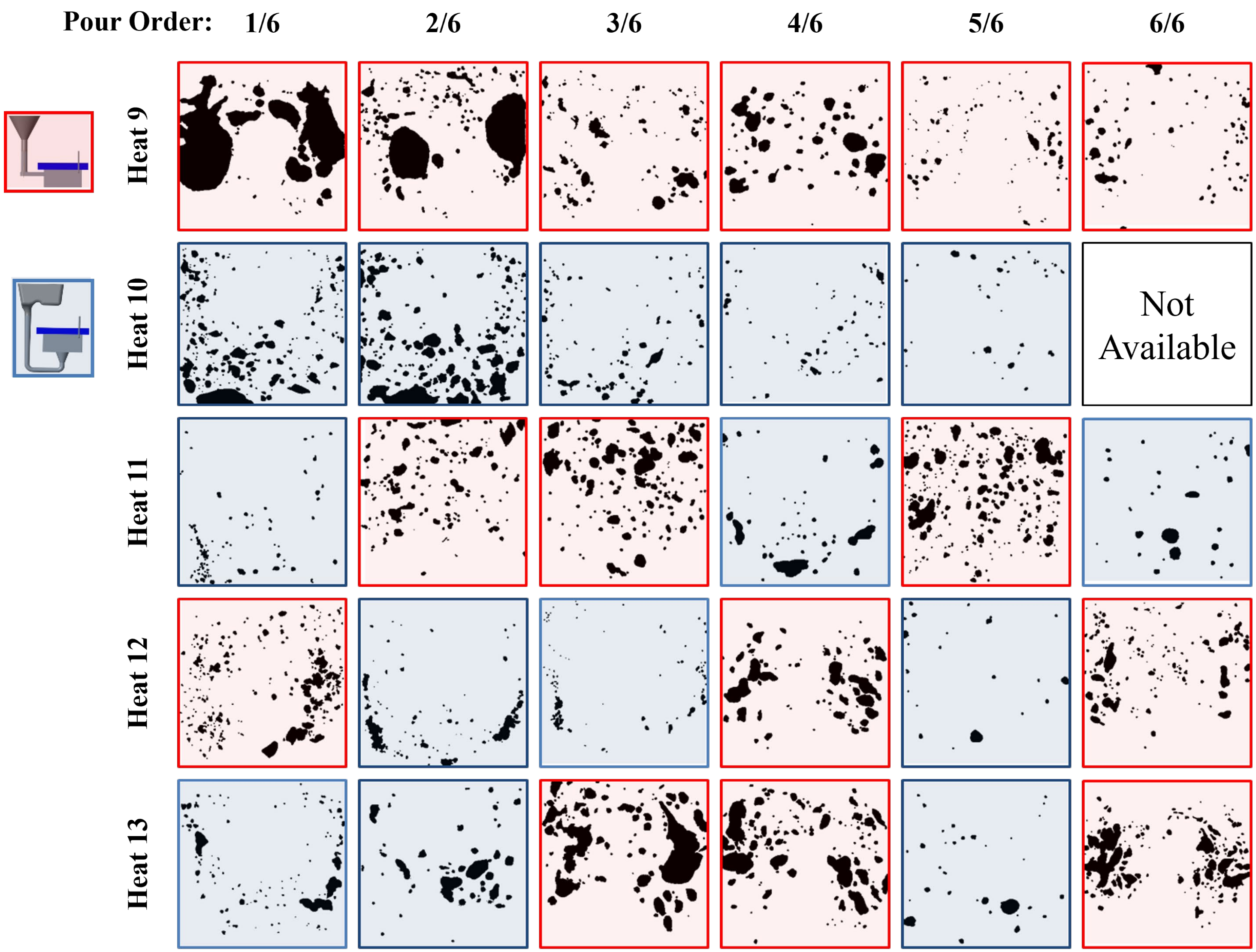

Figure 8. Measured inclusion maps for all 36 castings obtained using inclusion measurement Method 2. Case A castings have a red frame and background, while Case E castings are marked in blue.

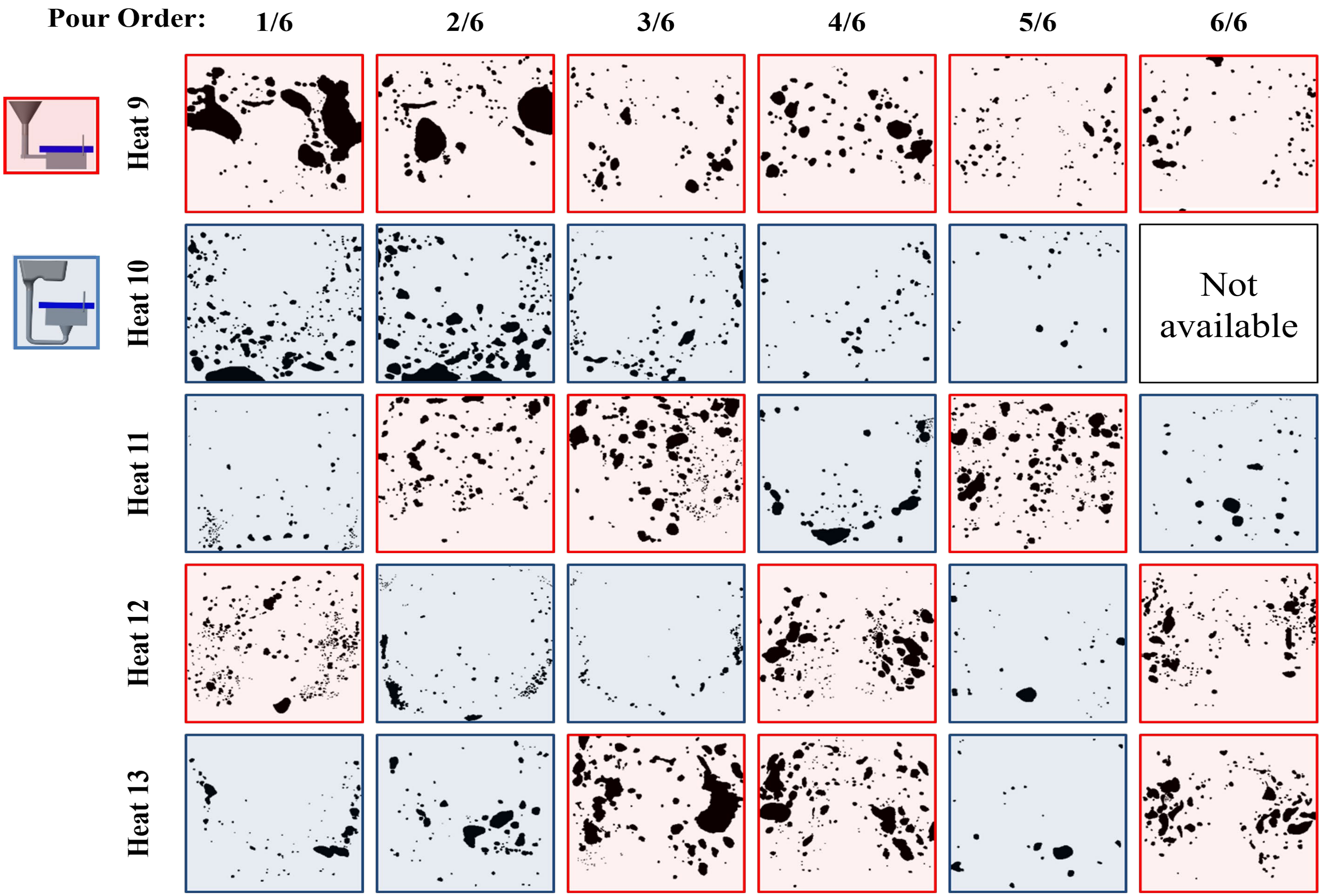

Figure 9. Measured inclusion maps for all 36 castings obtained using inclusion measurement Method 3. Case A castings have a red frame and background, while Case E castings are marked in blue.

Case A

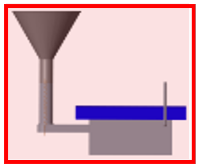

Case E

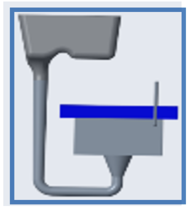

Percent surface covered with inclusions

Inspection method 2

	Pour Order					
Heat #	1	2	3	4	5	6
Heat 9	32.0	21.5	6.9	11.0	3.3	4.2
Heat 10	13.6	19.6	4.5	2.2	1.4	NA
Heat 11	2.3	9.2	14.7	5.7	15.6	3.1
Heat 12	9.5	4.6	1.9	11.0	1.4	7.4
Heat 13	5.1	6.9	21.5	14.7	2.4	13.6

Inspection method 3

	Pour Order					
Heat #	1	2	3	4	5	6
Heat 9	21.8	19.6	5.9	9.8	3.5	4.3
Heat 10	11.8	16.5	5.1	2.5	1.3	NA
Heat 11	2.2	8.1	14.9	6.9	14.0	3.0
Heat 12	7.7	3.7	1.7	12.1	1.9	8.5
Heat 13	3.0	6.1	18.4	14.7	2.1	10.6

Figure 10. Summary of inclusion area percentages for measurement Methods 2 and 3.

Statistical Analysis and Discussion

The inclusion area percentages summarized in Figure 10 were statistically analyzed to determine answers to the three questions in the Introduction. The results are provided in Figures 11 to 13. In general, inclusion measurement Methods 2 and 3 give similar results. Method 3 usually results in slightly lower area percentages than Method 2, but these differences are well within the standard deviations of the measurements.

Figure 11 shows a direct comparison of Cases A and E. The mean inclusion area percentage for all 18 Case A castings is approximately 2.5 times as large as the mean for all 18 Case E castings. Hence, the gating system for Case E is significantly better than the one for Case A. However, even Case E still has a 5% inclusion area coverage on the average, with the upper limit of the standard deviation being as high as 10%. Based on the standard deviations, the best Case A casting can easily be cleaner than the worst Case E casting. This emphasizes the need to cast a large number of castings (36 total in the present study) before making definite conclusions regarding the improvements a particular gating system has to offer. Based on the results of our previous study [3] discussed in the Introduction, the reduction in inclusions that the Case E gating system provides relative to Case A should not be attributed to fewer inclusions being generated inside of the gating system. Instead, the gating system for Case E simply traps more of the inclusions coming from the ladle. It was observed during pouring of the Case E castings that a fairly large amount of "dirt" or slag from the ladle stays in the pour basin and never enters the sprue. This is not the case when using a standard pouring cup as in Case A.

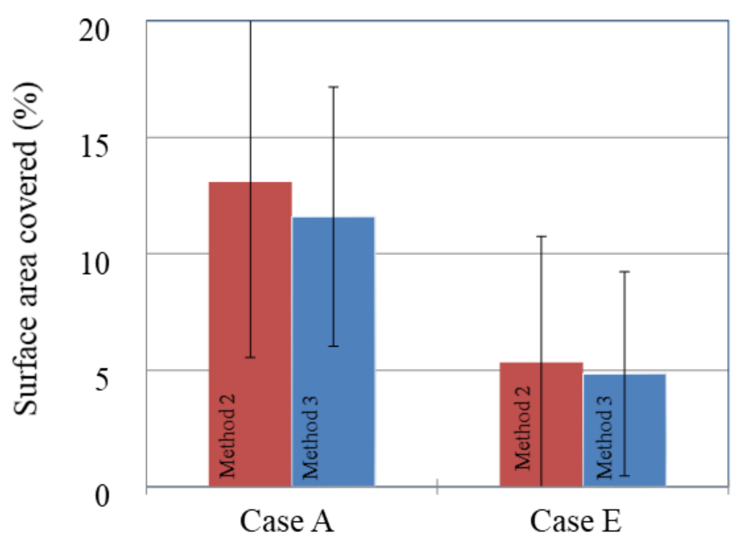

Figure 11. Comparison of the measured inclusion area percentages between all Case A and Case E castings. The bars are the means of the area percentages for each case, while the vertical lines represent the standard deviation. The red and blue bars correspond to inclusion measurement Methods 2 and 3, respectively.

The effect of pour order on casting cleanliness is examined in Figure 12. For the Case A castings, the inclusion area percentage decreases steadily from a mean of about 20% in Figure 12(a) and 15% in Figure 12(b), depending on the measurement method, for the first casting poured from the ladle to about 8% for the last (6^{th}) casting poured. This decrease can only be explained by the cleanliness of the melt from the ladle improving as the ladle is emptied. The oxides in the ladle will typically float to the top and leave with the pouring stream over the lip of the tilt pour ladle used in the present study. As more castings are poured, there are fewer oxides left in the ladle and the melt cleanliness improves. For the Case E gating system, however, the casting cleanliness is not a strong function of pour order. The first two Case E castings in a heat are, on average, about twice as dirty as the last four, but the decrease in the inclusion area percentage with pour order is not progressive. This can be explained by the pour basin used in the Case E gating system. The pour basin traps a large portion of the oxides coming initially from the ladle. In particular for the first pour, the Case E castings have an inclusion area percentage that is about three times smaller than for Case A.

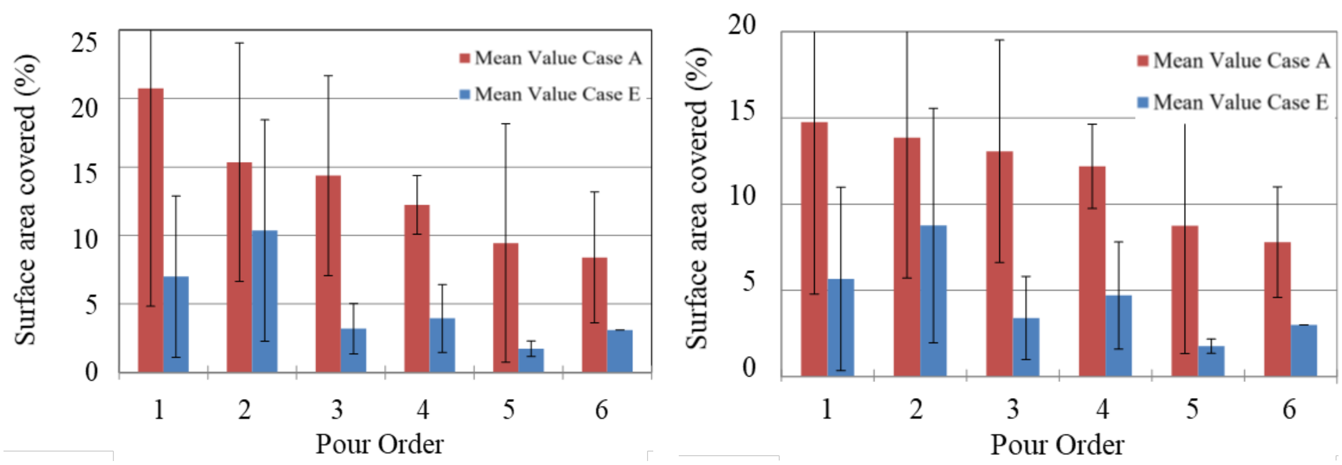

(a) (b)

Figure 12. Effect of pour order on the inclusion area percentage. The red and blue bars are the means for the Case A and E castings, respectively, and the vertical lines represent the standard deviation. The left graph (a) is for inclusion measurement method 2, while the right graph (b) is for Method 3.

Heat to heat variations in casting cleanliness are analyzed in Figure 13(a) for measurement Method 2 and Figure 13(b) for measurement Method 3. It can be seen that there are no significant differences in inclusion area percentages between the six heats poured in the present study given that all standard deviation bars encompass all the measured mean values. This is expected since the heats were all prepared in the same way.

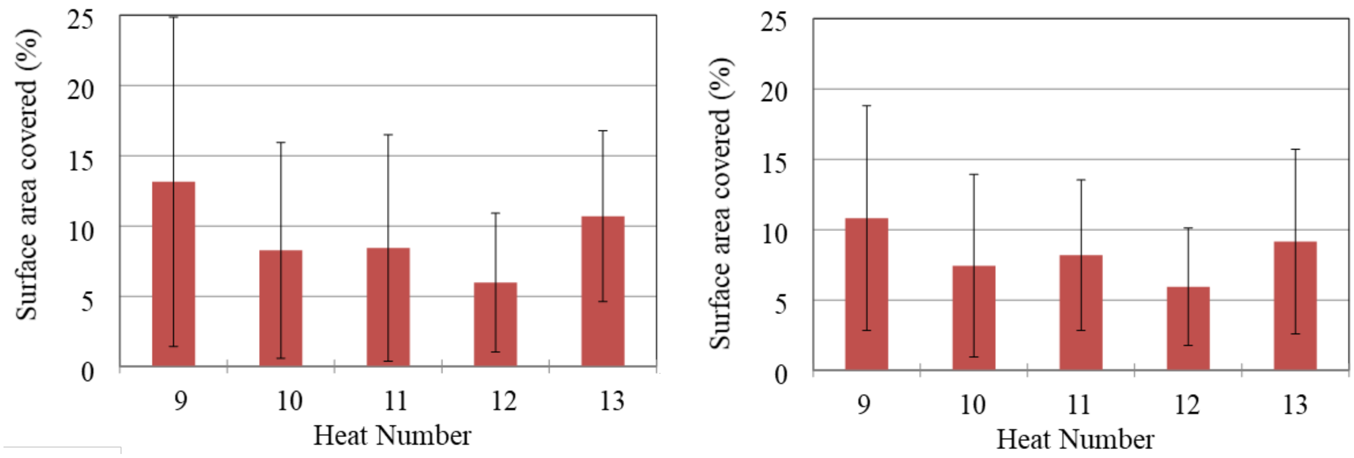

(a) (b)

Figure 13. Effect of heat number on inclusion area percentage. The red bars are the means for all six castings (Cases A and E) in a heat, and the vertical lines represent the standard deviation. The left graph (a) is for inclusion measurement method 2, while the right graph (b) is for Method 3.

Conclusions

Casting experiments were performed to investigate the effect the gating system and pour order on casting cleanliness. Two different gating systems are selected from a previous study. The first gating system is poor (Case A) and employs a standard pouring cup, oversized sprue and runner, and a side ingate near the top. When filling the poor system, the downsprue never fills and there is a water fall into the casting; both result in splashing and mixing of air and steel. The second gating system (Case E) is more sophisticated and features an offset pouring basin, a tapered sprue, streamlined runner connections, and a tapered bottom ingate. This system fills smoothly with almost no air/steel mixing. The questions to be answered by the study were: 1) what is the actual improvement in casting cleanliness when switching from the poor to the sophisticated gating system, 2) what is the effect of pour order on casting cleanliness when using a standard tilt pour ladle, and 3) how much does the casting cleanliness vary between different heats.

In answering the first question, it was found that the more sophisticated gating system offers a 2.5 times improvement in the inclusion area percentage relative to the poor gating system. This is attributed to more of the oxides from the ladle being trapped by the pouring basin and the rest of the gating system.

Answering the second question, the poor gating system results in a strong dependence of the casting cleanliness on the pour order, with the first casting having an inclusion area percentage that is about twice as high as the sixth. This dependency is much reduced for the sophisticated gating system. For the poor gating system (Case A) castings, the inclusion area percentage decreases steadily from a mean of about 20% and 15% for the first casting poured, depending on measurement method, to about 8% for the last casting poured. This decrease is explained by the cleanliness of the melt from the ladle improving as the ladle is emptied. Oxides in the ladle typically float upwards and leave with the pouring stream over the lip of the ladle used in the present study. As more castings are poured, there are fewer oxides left in the ladle and the melt cleanliness improves. For the sophisticated gating system (Case E), the casting cleanliness is relatively insensitive to pour order. The first two Case E castings in a heat are, on average, about twice as dirty as the last four, but the decrease in the inclusion area percentage with pour order is not progressive. This is explained by the pour basin used in the Case E gating system, which traps a large portion of the oxides coming from the ladle. In particular for the first pour, the Case E castings have an inclusion area percentage that is about three times smaller than for Case A.

Addressing the third question, heat to heat variations in casting cleanliness are found to be negligibly small in this study. The heat to heat variations in casting cleanliness for both inclusion area measurement methods reveal no significant differences in inclusion area percentages between the six heats poured, given that all the measured mean values for each heat are within the variations of all heats, as represented by their standard deviations. All heats were prepared in the same way, so this is an unsurprising result.

The findings from this study support those from the earlier study. It is found that the primary source of inclusions is from the ladle. However, this is not to say that the gating system has no effect on inclusions in a casting. The gating system still appears to have two effects on casting cleanliness. Firstly, the gating system can "filter" out inclusions from the ladle if they float out of it, or get stuck and trapped inside the gating system prior to entering the casting. Secondly, inclusions are not evenly distributed in steel castings, and the geometry of the gating system will affect their distribution in the casting and final locations.

Acknowledgements

This research is sponsored by the DLA-Troop Support, Philadelphia, PA and the Defense Logistics Agency Information Operations, J68, Research & Development, Ft. Belvoir, VA. The authors also recognize Sairam Ravi and his team at the University of Northern Iowa Metal Casting Center for pouring the casting experiments.

Disclaimer

References

[1] J.M. Svoboda, R.W. Monroe, C.E. Bates and J. Griffin, "Appearance and Composition of Oxide Macroinclusions in Steel Castings," AFS Transactions, Vol. 95, pp. 187-202, 1987

[2] J.A Griffin and C.E. Bates, “Ladle Treating, Pouring and Gating for the Production of Clean Steel Castings,” Steel Founders' Society of America Research Report No. 104, 1991.

[3] Donahue, R., Hardin, R., and Beckermann, C., "Effects of Gating System and Casting Geometry on Oxide Inclusions in Steel Castings," in Proceedings of the 75th SFSA Technical and Operating Conference, Paper No. 4.11, Steel Founders' Society of America, Chicago, IL, 2021.

[4] Schindelin, J., Arganda-Carreras, I., and Frise, E. et al., "Fiji: An Open-Source Platform for Biological-image Analysis", Nature Methods, Vol. 9, No. 7, pp. 676-682, 2012.